Journal of ELECTRONIC MATERIALS, Vol. 38, No. 11, 2009
DOI: 10.1007/s11664-009-0888-y

Regular Issue Paper

Wetting Behavior and Mechanical Properties of Sn-Zn and Sn-Pb Solder Alloys

LEONARDO R. GARCIA,[1] WISLEI R. OSÓRIO,[1] LEANDRO C. PEIXOTO,[1] and AMAURI GARCIA[1,2]

1.—Department of Materials Engineering, University of Campinas, UNICAMP, P.O. Box 6122, 13083-970 Campinas, SP, Brazil. 2.—e-mail: amaurig@fem.unicamp.br

A comparative experimental study of the main features of the eutectic Sn-Pb alloy and Sn-Zn alloys was carried out with a view to application of the latter alloys as alternative solder materials. The resulting microstructures, mechanical properties (ultimate tensile strength and elongation), and wettability behavior (spreading area and contact angle) of a hypoeutectic Sn-Zn (Sn-4wt.%Zn), a hypereutectic Sn-Zn (Sn-12wt.%Zn), and the eutectic Sn-9wt.%Zn alloy were examined and compared with the corresponding results of the conventional Sn-40wt.%Pb solder alloy. It was found that, of the Sn-Zn alloys examined, the eutectic Sn-9wt.%Zn alloy offers a compromise between lower wettability and higher mechanical strength.

Key words: Sn-Zn solder alloys, wettability, hot-dipping, mechanical properties, cooling rate, solidification

INTRODUCTION

Due to the rapid development of electronic and communication components in the past few decades, Sn-Pb solder has been the most dominant material for interconnection, packaging of modern electronic components, temperature-sensitive components, optoelectronics modules, step soldering processes, and printed circuit or wiring boards.[1–3] Lead-containing solders, particularly Sn-Pb alloys, have also played an important role in a number of other industrial applications, such as water piping, food and beverage cans, and automobile bodies.[4–7] However, lead and lead-containing compounds are considered toxic due to their detrimental effect on the well-being of humans and the environment. Suitable development policies have been implemented by many countries around the world and, in order to protect the environment, the restriction of lead use in industry has been strongly promoted. In this context, since July 1, 2006, both the European Union (RoHS—Restriction of Certain Hazardous Substances) and the US Environmental Protection Agency have banned lead-containing electronic products.[4]

Great efforts to replace traditional Sn-Pb eutectic solder alloy with lead-free alternatives are underway. Melting temperature has become an important reference point for the development of Pb-free solder alloys.[1,7] The nontoxic Pb-free solder alternative that has a melting temperature closest to that of the eutectic Sn-Pb alloy is the Sn-Zn eutectic alloy (183°C and 198°C, respectively).[1,3–7] However, new solder alloys must fulfill a number of other requirements from both economic and physical/chemical points of view.[8,9] In this context, the melting temperature should be in the same range as that of the traditional Sn-Pb eutectic alloy, strength and integrity should also be similar or superior, and manufacturing costs must be competitive.

Considering performance, reliability, cost, and resources, alloys from the Sn-Zn, Sn-Ag, Sn-Bi, Sn-Cu, Sn-Cd, Sn-Au, and Sn-Sb binary systems are being considered as promising lead-free solder alloys.[5–11] A number of studies[11–14] have also been focused on alloys of multicomponent systems such as Sn-Zn-Ag,[12] Sn-Ag-Cu,[13,14] Sn-Zn-In,[15] Sn-Zn-Bi,[16,17] Sn-Zn-Ag-Al, and Sn-Zn-Ag-Al.[7] However, these solder alloys require accurate preparation in terms of chemical composition and

(Received April 28, 2009; accepted June 19, 2009; published online August 4, 2009)

some modifications of existing production plants due to their higher melting temperatures compared with the Sn-Pb eutectic alloy. Some other operational aspects have limited the adoption of these candidate replacements for Pb-free alloys for certain soldering applications.[3] For flip-chip or ball-grid-array (BGA) joint technologies,[7,17] it is expected that the resulting surface microstructure, composition, and properties can unintentionally and considerably differ from those of the nominal composition when multicomponent alloys are used. Considering these limitations, binary alloys are preferred, particularly Sn-Zn alloys, because it is expected that they will enable existing production lines to be used without any modification. Benefit can also be attained due to the mechanical integrity provided to electronic packaging, manufacturability, and relatively low cost.[4,17] In contrast, Suganuma and Kim[3] reported that the application of Sn-Zn alloys as Pb-free solder has some drawbacks, such as poor oxidation resistance in high-temperature/humidity conditions and poor compatibility with Cu substrates at elevated temperature.

It is well known that solder joints are subjected to thermal stresses and strains during operation, which can produce distortions at the joint[18] or excess heating during reflow treatment, inducing damage to electronic devices or decreasing their lifetime in the long term.[3] As temperature variations can provide stress and strain within the joint, if the mechanical properties of the solder alloy are known, these values can be used in mathematical models to predict the reliability and lifetime of the solder joint.[18]

Although the metallurgical and micromechanical aspects of the factors controlling microstructure, unsoundness, strength, and ductility of solder alloys are complex, it is well known that thermal processing variables play an extremely important role.[19–24] In particular, information correlating the mechanical properties of Sn-Zn alloys with the resulting microstructure cannot be found in the literature. Islam et al.[4] reported that solder joint formation is also strongly dependent on how well the solder alloy can wet the substrate. Wetting balance test (contact or wetting angle measurement), spread test, solder ball, slump test, and ball shear test are the most common standard procedures carried out in order to characterize the wettability of solder alloys on substrates.[4,17,25]

The present work is a comparative experimental study focusing on the main features of the eutectic Sn-Pb alloy and Sn-Zn alloys, with a view to application of the latter alloys as alternative solder materials. The resulting microstructures, mechanical properties (ultimate tensile strength and elongation), and wettability behavior (spreading area and contact angle) of a hypoeutectic Sn-Zn (Sn-4wt.%Zn), a hypereutectic Sn-Zn (Sn-12wt.% Zn), and a eutectic Sn-9wt.%Zn alloy were examined and compared with the corresponding results of the conventional Sn-40wt.%Pb solder alloy.

EXPERIMENTAL PROCEDURES

Sn-Zn and Sn-Pb solder alloys samples were prepared from commercially pure metals, as described in Table I. A hypoeutectic Sn-4wt.%Zn, a eutectic Sn-9wt.%Zn, a hypereutectic Sn-12wt.%Zn alloy, and the traditional eutectic Sn-40wt.%Pb alloy were melted in an electric-resistance-type furnace, and the molten alloy was stirred for adequate homogenization before pouring into a casting mold.

Alloy Droplets

The aforementioned castings were remelted and sessile drops of about 2 g for each studied alloy were deposited on three different substrates: copper, low-carbon SAE 1020 steel, and a commercial tin plate (with thickness of about 150 μm on low-carbon steel) under two different melt superheats (50°C and 100°C above the alloy liquidus temperature). Both superheat and substrate materials were chosen in order to simulate various industrial applications. The substrates were sequentially degreased in a 5 wt.% NaOH solution at room temperature for 15 s, followed by rinsing in an HCl (5 vol.%) solution, and finally washed in deionized water for 10 s. Each solidified alloy drop image was acquired by using an image processing system (stereomicroscope SZ 40 Olympus and Image-Pro Express software from Media Cybernetics, version 5.1.0.12). Contact angles (Fig. 1) were measured using ImageJ®.

Table I. Chemical Compositions of Zn, Sn, and Pb Used to Prepare the Solder Alloys

Chemical composition of Zn					
Element	Zn	Fe	Al	Pb	Other
wt.%	99.995	0.003	0.002	<0.001	<0.001
Chemical composition of Sn					
Element	Sn	Fe	Pb	Si	Other
wt.%	99.991	0.005	<0.001	0.003	<0.001
Chemical composition of Pb					
Element	Pb	Fe	Al	Si	Other
wt.%	99.57	0.41	<0.001	0.023	<0.001

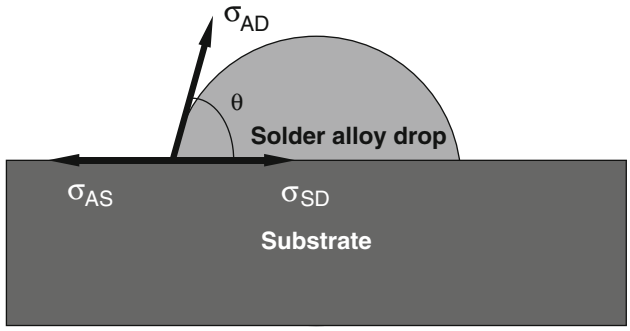

Fig. 1. Schematic representation of the contact angle (θ) between an alloy drop and a substrate, where σ_{AS}, σ_{AD}, and σ_{SD} refer to the surface tensions of liquid/environment, substrate/environment, and liquid/substrate, respectively.

Six samples of each alloy were evaluated in order to obtain an average result.

Hot-Dipping

For this procedure, Cu plates with approximate dimensions of 150 mm × 20 mm × 1.5 mm, degreased in NaOH and HCl solutions, were used. The Cu plates (substrates) were immersed into the three studied Sn-Zn and eutectic Sn-Pb molten alloys, which were kept at different temperatures (300°C, 250°C, 230°C, and 210°C; ±2°C) under air atmosphere. The dipping rates were about 12 mm/s to 15 mm/s (close to those used in similar procedures carried out by Yu et al.[1] and Lin et al.[7]); dipping time was about 3 s, and the corresponding dipping depth was 70 mm. A schematic representation of the dipping procedure is shown in Fig. 2a. The spread areas were obtained by analyzing the corresponding optical photograph using ImageJ® software and the average recovered area was determined. The thickness of each alloy layer deposited on the Cu substrate was also measured by using the optical images in transverse section, as shown in Fig. 2b.

The resulting microstructures of the deposited layers were acquired by using an image processing system Neophot 32 and Cambridge Leica 500, which was also used to measure the secondary dendrite arm spacing.

Microstructure

The alloy specimens were ground, polished, and etched to reveal the microstructure by using a solution of 92 vol.% CH_3OH, 5 vol.% HNO_3, and 3 vol.% HCl for 5 s. The secondary dendrite arm spacing (λ_2) was measured by averaging the distance between adjacent side-branches on the longitudinal section of a primary dendritic arm (20 λ_2 values were measured for each selected position).

Tensile Testing

In order to evaluate the mechanical properties associated with the microstructures attained in hot-dipping tests, specimens with similar resulting microstructures (similar cooling rates) were obtained and prepared for tensile testing according to specifications of ASTM standard E 8M/04 and tested in a MTS Test Star II machine at a strain rate of about 1×10^{-3} s^{-1}. A schematic representation of the shape and dimension of the tensile testing specimens as well as the location from which they were extracted from the casting is shown in Fig. 3. In order to ensure reproducibility of the tensile results, three specimens were tested for each selected position. A water-cooled vertical

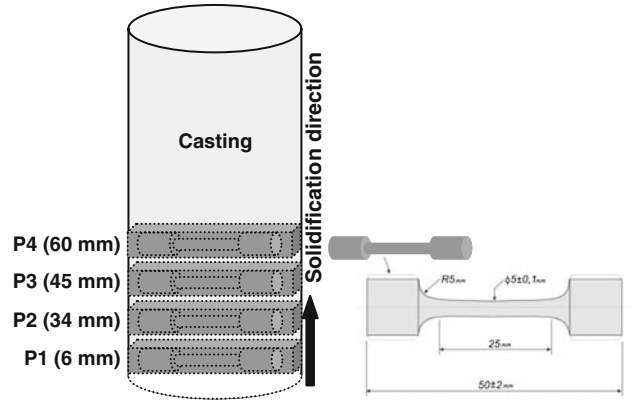

Fig. 3. Schematic representation with dimensions and location of specimens for tensile testing.

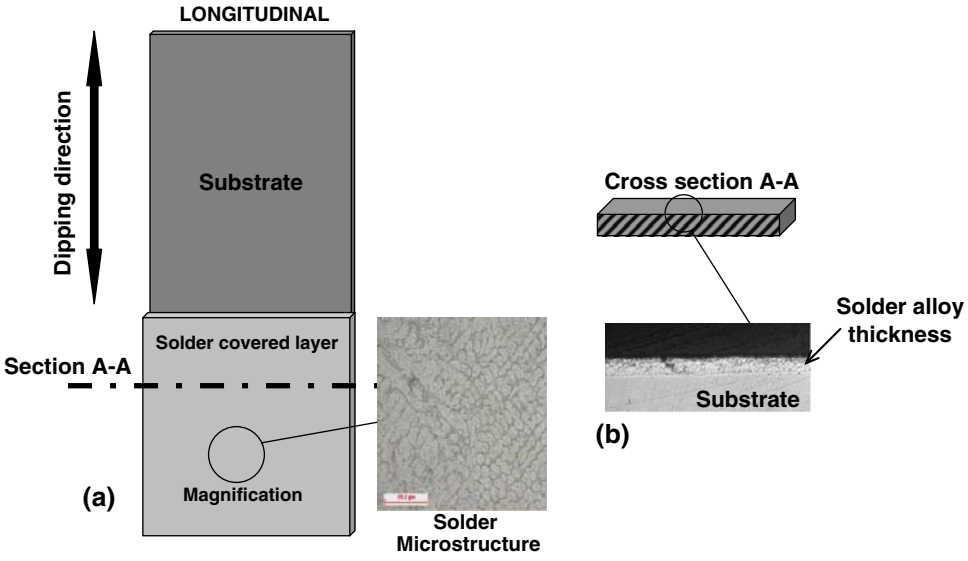

Fig. 2. Schematic representation of the dipping test to obtain: (a) average spread area on Cu substrate and corresponding microstructure and (b) thickness of the covered layer in a cross-section.

upward unidirectional solidification system was used to obtain the specimens. The mentioned solidification system was designed in such a way that the heat was extracted only through the water-cooled bottom, promoting upward directional solidification, as detailed in previous articles.[24–27] Specimens for tensile tests were withdrawn at specific regions (positions) along the casting associated with particular cooling rates.

RESULTS AND DISCUSSION

Wetting Angle

The contact or wetting angle (Fig. 1) at which the oval of a drop of liquid metal contacts the substrate surface determines the chemical affinity between the two substances, i.e., a flat drop (small wetting angle) indicates high affinity and in this case the liquid is said to wet the substrate. Experimental results of contact angles on the copper substrate as a function of melt superheat (50°C and 100°C above the liquidus and the eutectic temperatures) for the Sn-4wt.%Zn, Sn-12wt.%Zn, Sn-9wt.%Zn, and Sn-40wt.%Pb alloys are shown in Fig. 4. It is important to remark that the shape of the sessile drops of the Sn-Zn alloys was not perfectly ellipsoidal but irregular in about 10% of the experimental drops. These irregular drops were not considered for determination of average values of wetting angles. These irregular shapes can be associated with oxidation. The presence of surface-active elements such as oxygen will have a significant influence on measurements of contact angle. The formation of a zinc oxide film can provoke drop surface distortions. Atmospheric oxygen molecules pass through this oxide and promote a diffusion reaction within the solder to form a thick oxide layer. Suganuma et al.[28] have also reported that sessile drops can be distorted due to oxidation, preventing the solders from uniform wetting and spreading.

The contact angles on the Cu substrate for all alloys examined generally tended to attain their lowest values for a melt superheat of 100°C, as can be seen in Fig. 4. However, based on the range of values of contact angles given by the error bars (maximum and minimum values), average values of about 59° and 48° can be considered for the three Sn-Zn alloys and the Sn-40wt.%Pb solder alloy, respectively. Wu et al.[29,30] also reported that contact angle decreases with increasing melt temperature, which is associated with lower viscosity and consequent better metal/substrate wetting. These results are in agreement with viscosity results reported by Toye and Jones.[31] Although in the present study the wetting tests were carried out without application of flux, as is usual in industrial practice, the determined experimental contact angles are similar to those reported by Islam et al.,[4] Wu et al.,[30] and Cheng and Li.[32]

Comparisons of contact angles at soldering temperatures with melt superheats of 50°C and 100°C on low-carbon steel (SAE 1020) and tin plate substrates are shown in Figs. 5 and 6, respectively. The average values of contact angles on both low-carbon steel and tin plate substrates for the Sn-4wt.%Zn, Sn-12wt.%Zn, and Sn-40wt.%Pb alloys seem not to be significantly affected by the melt superheat. On the other hand, for the eutectic Sn-9wt.%Zn alloy a decrease (of about 17%) in the contact angle at 100°C can be observed when compared with that attained for a 50°C melt superheat, as shown in Figs. 5 and 6. Lower contact angles are associated with higher fluidity. It has been demonstrated that best fluidity is generally attained for pure components, eutectics or phases that freeze congruently, whereas fluidity decreases with increasing solidification range.[33] This seems to be the case for the

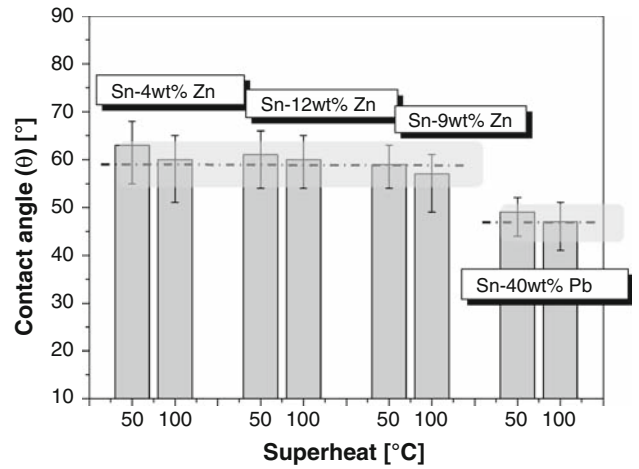

Fig. 4. Experimental results for contact angles on the copper substrate as a function of melt superheat (50°C and 100°C above the liquidus and eutectic temperatures) for the Sn-4wt.%Zn, Sn-12wt.%Zn, Sn-9wt.%Zn, and Sn-40wt.%Pb solder alloys.

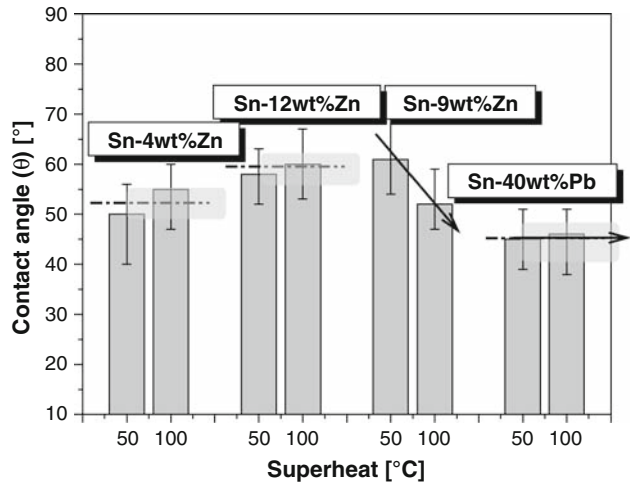

Fig. 5. Experimental results of contact angles on the low-carbon steel substrate as a function of superheat (50°C and 100°C above the liquidus and eutectic temperatures) for the Sn-4wt.%Zn, Sn-12wt.%Zn, Sn-9wt.%Zn, and Sn-40wt.%Pb solder alloys.

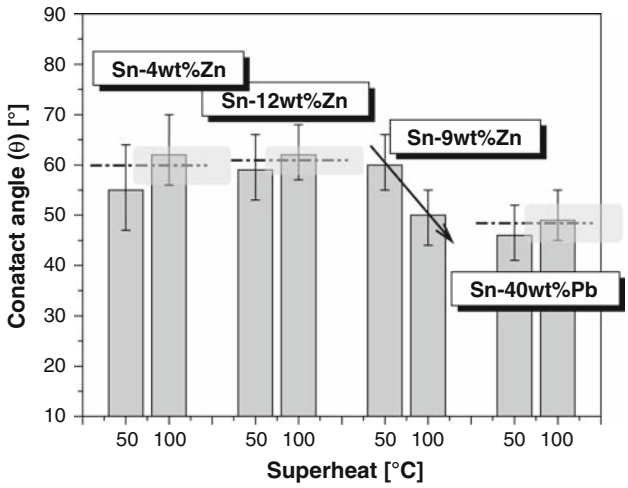

Fig. 6. Experimental results of contact angles on the tin plate substrate as a function of superheat (50°C and 100°C above the liquidus and eutectic temperatures) for the Sn-4wt.%Zn, Sn-12wt.%Zn, Sn-9wt.%Zn, and Sn-40wt.%Pb solder alloys.

observed differences between eutectic and noneutectic Sn-Zn alloys for a melt superheat of 100°C.

Comparing the experimental results of contact angle for all the studied alloys for the copper, low-carbon steel, and tin plate substrates, it can be observed that the Sn-40wt.%Pb solder alloy has a similar average contact angle of about 45°. The Sn-4wt.%Zn solder alloy has its lowest contact angle (average value of about 52°) on the low-carbon steel substrate. The Sn-9wt.%Zn alloy exhibited minimum values of contact angle of about 50° for the low-carbon steel and tin plate substrates. From these experimental observations, it can be said that, in the search for alternatives to replace the traditional Sn-40wt.%Pb solder alloy, experimental results encompassing both the nature of the substrate and the melt superheat should be considered.

Coating Layer: Spread Area and Thickness

Despite the use of a number of different substrates in several industrial fields, in the present study dipping tests were only carried out on Cu plates. This substrate was chosen due to its wide commercial application. The dipping tests were carried out at four different melt (or dipping) temperatures (300°C, 250°C, 230°C, and 210°C) with a dipping rate of about 12 mm/s to 15 mm/s in order to simulate the range of soldering temperatures applied in industrial processes. Typical photographs of as-dipped Sn-Zn solder alloys on copper substrates at these dipping temperatures are shown in Fig. 7. The spread areas were obtained by analyzing the optical photographs furnished by using the ImageJ® software, and average values of coverage as a function of dipping temperatures were determined and are reported in Table II. It is known that the coverage (%) is strongly dependent on the wettability of the solder alloy on each substrate and is also affected by viscosity. Low viscosity provides poor solder/substrate adhesion. It can be observed that the Sn-9wt.%Zn alloy at 210°C and 230°C yielded slightly better coverage than the Sn-40wt.%Pb alloy. At 250°C, which is a usual soldering temperature in industrial processes,[1,28–32] similar coverage can be observed, of the order of 98.7% for both eutectic alloys. The Sn-Zn alloys had lower coverage compared with the Sn-Pb alloy only

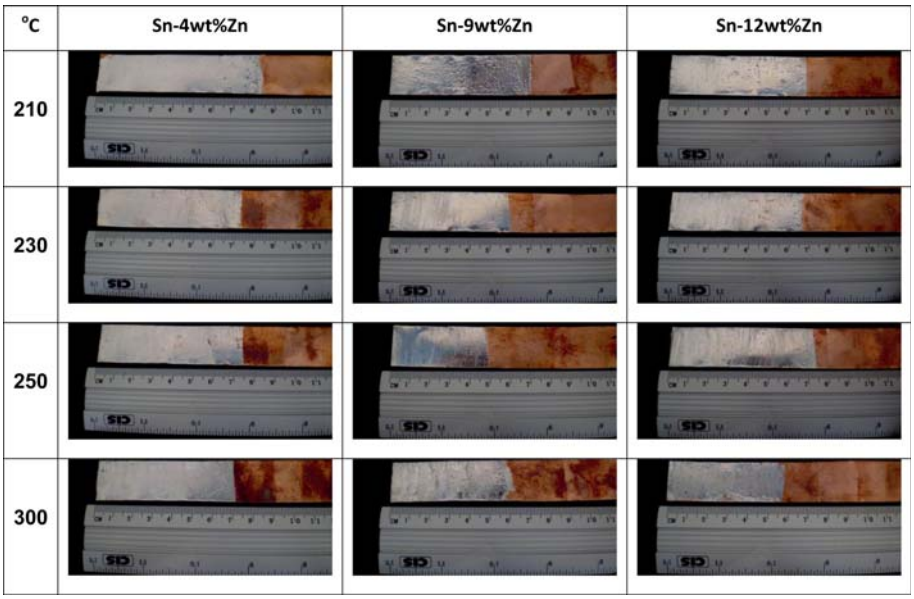

Fig. 7. Typical photographs of as-dipped Sn-4wt.%Zn, Sn-9wt.%Zn, and Sn-12wt.%Zn solder alloys on a copper substrate (molten alloys at 210°C, 230°C, 250°C, and 300°C).

Table II. Percentage of Covered Area as a Function of Four Different Dipping Temperatures

Solder Alloy	Dipping Temperature (°C)	Covered Area (%)
Sn-4wt.%Zn	210	98.3 ± 0.5
	230	98.1 ± 0.3
	250	97.5 ± 0.4
	300	96.9 ± 0.5
Sn-9wt.%Zn	210	99.0 ± 0.2
	230	98.9 ± 0.5
	250	98.7 ± 0.4
	300	98.7 ± 0.2
Sn-12wt.%Zn	210	97.4 ± 0.5
	230	98.7 ± 0.2
	250	98.8 ± 0.5
	300	95.0 ± 0.7
Sn-40wt.%Pb	210	98.3 ± 0.2
	230	99.0 ± 0.4
	250	98.7 ± 0.4
	300	99.0 ± 0.3

at the dipping temperature of 300°C, as shown in Table II. These results confirm that, considering the resulting coverage, a eutectic Sn-9wt.%Zn solder alloy can be considered a potential lead-free solder replacement.

Figure 8 shows the resulting cooling curves acquired during the hot-dipping tests, for both the Sn-9wt.%Zn and Sn-40wt.%Pb eutectic solder alloys after 3 s of dipping at 300°C, 250°C, 230°C, and 210°C. It is important to remark that curves of temperature versus time in dipping-in (heating) are not presented. The cooling rates were determined for all four different hot-dipping temperatures, and an average cooling rate of about 12°C/s was established for both the Sn-9wt.%Zn and the Sn-40wt.%Pb alloys before the eutectic reaction. The subsequent cooling after solidification, for both Sn-Zn and Sn-Pb eutectic solder alloys, was shown to proceed under an average cooling rate of about 6°C/s, for any hot-dipping temperature, as shown in Fig. 8.

Microphotographs of cross-sections evidencing the resulting thicknesses of the areas covered by each alloy on the copper substrate after hot-dipping tests at temperatures of 300°C, 250°C, 230°C, and 210°C are shown in Fig. 9. The thicknesses of the covered areas as a function of dipping temperatures are shown in Fig. 10. It is observed that only the Sn-Pb solder alloy tends to have the covered layer thickness decreasing with increasing dipping temperature, as shown by the shaded region. On the other hand, all Sn-Zn solder alloys experienced a slight increase in layer thickness with increasing dipping temperature, as shown in Fig. 10. In the range of dipping temperatures between 230°C and 250°C, quite similar covered layer thicknesses for all solder alloys are observed. Recently, Wei et al.[34] using a hypoeutectic Sn-Zn alloy as lead-free solder material, reported that the layer thickness

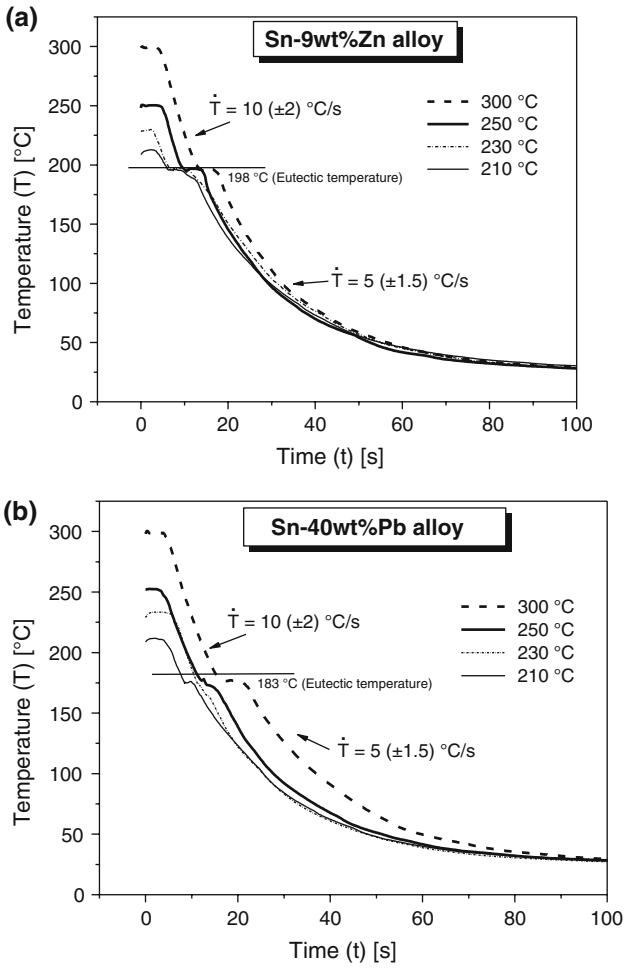

Fig. 8. Typical cooling curves obtained in the hot-dipping tests for: (a) eutectic Sn-9wt.%Zn and (b) Sn-40wt.%Pb solder alloy after 3 s of dipping at 300°C, 250°C, 230°C, and 210°C.

increases with increasing Zn content. This tendency has been observed in the present experimental investigation only for dipping temperatures higher than 250°C. The solidification of thin layers is a process in which the thermal resistance at the metal/substrate interface is dominant. This means that the solidified thickness will be strongly dependent on the heat transfer coefficient, h, at this interface.[35] On the other hand, higher wettability is generally provided by higher dipping temperatures, which will increase h, thus favoring the growth of thicker layers. As the dipping process is carried out vertically, good adhesion of the liquid layer to the substrate must also be accomplished to assure an increase in wettability with dipping temperature. The association of increasing wettability and adhesion with increasing dipping temperature and alloy Zn content could explain the present observed results for the Sn-Zn alloys.

Suganuma et al.[28] have also reported that the thicknesses of the covered areas of hypoeutectic Sn-3wt.%Zn and Sn-6wt.%Zn solder alloys increase with increasing soldering temperature. They have

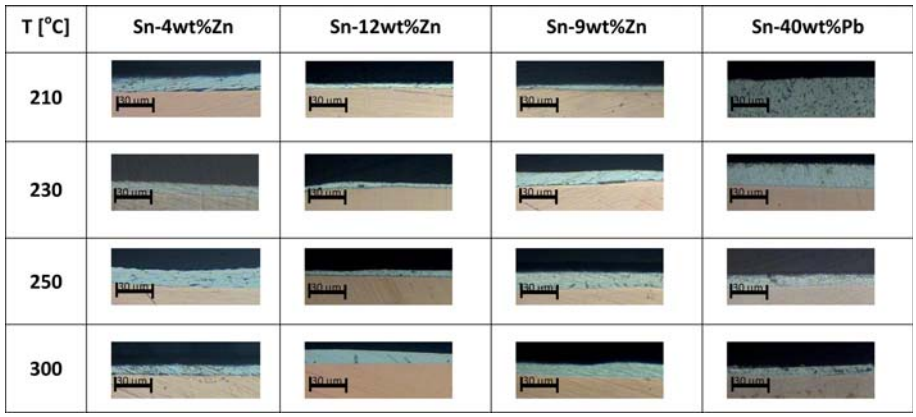

Fig. 9. Microphotographs of the cross-section, showing the resulting thicknesses of covered areas on copper substrate after hot-dipping tests at dipping temperatures of 300°C, 250°C, 230°C, and 210°C.

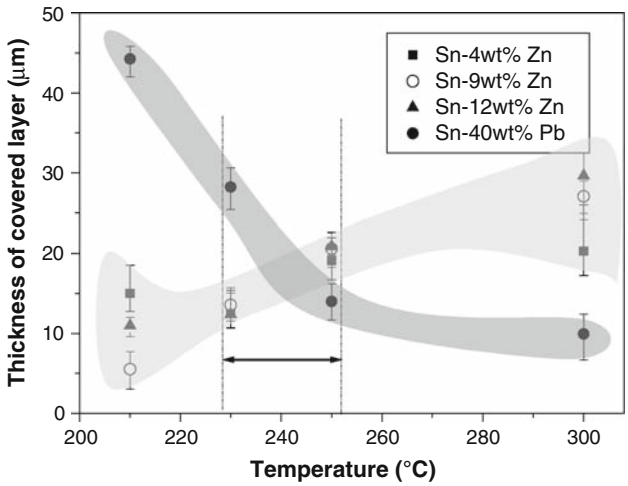

Fig. 10. Thicknesses of covered layer of Sn-4wt.%Zn, Sn-9wt.%Zn, Sn-12wt.%Zn, and Sn-40wt.%Pb solder alloys as a function of dipping temperature, showing two different shaded regions for trends of thickness evolution for Sn-Zn and Sn-Pb alloys.

also observed that, for all soldering temperatures examined, the smallest thickness was that of the Sn-3wt.%Zn alloy, i.e., for the alloy with lower Zn content.

Microstructure and Tensile Tests Results

In order to evaluate the mechanical properties associated with the microstructures resulting from the hot-dipping procedure, specimens with similar cooling rates (similar microstructures) were obtained. All hot-dipping tests for each alloy examined were carried out at a cooling rate of about 12 °C. The resulting microstructures were characterized by a secondary dendrite arm spacings of 8.5 ± 2 μm and 12 ± 2 μm for the Sn-4wt.%Zn and the Sn-12wt.%Zn alloys, respectively, as shown in Fig. 11. On the other hand, the Sn-9wt.%Zn eutectic solder alloy was characterized by a mixture of globular-like Zn particles having a diameter of about 5 μm in a Sn-rich matrix, as can also be seen in Fig. 11. It is well known that the cooling rate during solidification controls the resulting microstructure. In this context, Sn-4wt.%Zn and Sn-12wt.%Zn alloys can have coarser dendrite arrays if cast at lower cooling rates. A needle-like Zn-rich phase with a width of about 16 μm associated with the eutectic mixture was observed in a previous study with a Sn-9wt.%Zn solder alloy which was solidified under conditions of low cooling rate.[36]

Figure 12 shows the experimental stress-strain curves for the Sn-4wt.%Zn, Sn-12wt.%Zn, eutectic Sn-9wt.%Zn, and Sn-40wt.%Pb alloys corresponding to specimens with microstructures associated with cooling rates of about 12°C/s during solidification (similar to that attained in hot-dipping tests). The curves represent average results of tensile tests carried out with four different specimens. With the exception of the eutectic alloys, the results show a peculiar behavior, with an initial elastic region followed by a small viscoplastic plateau associated with a balance between work hardening and dislocation unpinning mechanisms.[37] The plateau is clearly defined in a range of strains between 1.5% to 14% and 1.5% to 16% for the Sn-4wt.%Zn alloy and the Sn-12wt.%Zn alloy, respectively. From the experimental results, it can be observed that the highest ultimate tensile strength (UTS) of about 60 MPa and the lowest elongation of about 30% were obtained for the Sn-9wt.%Zn solder alloy. This seems to be closely associated with the resulting mixture of small globular-like Zn particles and the eutectic mixture, which is a result of the high cooling rate imposed during solidification.[36] The present UTS result is higher than those recently reported by Kim et al.[38] and Suganuma and Kim[3] (50 MPa), Lee et al.[39] (53 MPa), and Chen et al.[5] (43 MPa), and this seems to be associated with differences in microstructure which are related to the cooling rate during casting. On the other hand, the Sn-4wt.%Zn, Sn-12wt.%Zn, and Sn-40wt.%Pb solder alloys attained similar ultimate tensile strengths, of about 30 ± 5 MPa, with elongation of about 40%, 50%, and 35%, respectively.

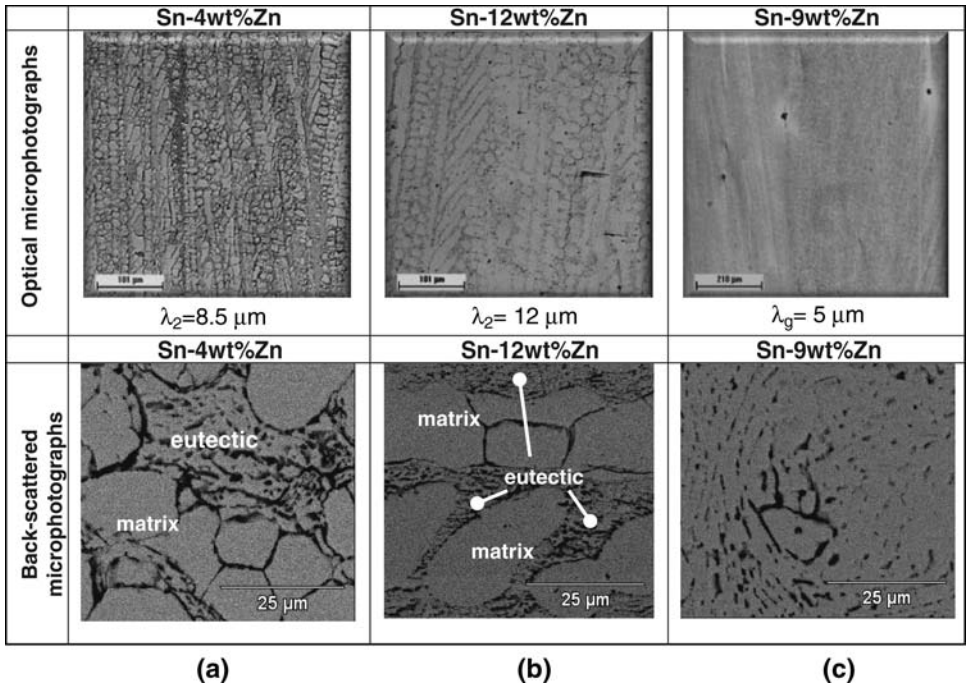

Fig. 11. Typical microstructures of Sn-Zn solder alloys at longitudinal sections of samples resulting from a cooling rate of about 12 °C/s. (a, b) Dendritic morphology (125× magnification); λ_2 is the average secondary dendrite arm spacing. (c) Globular-like Zn particles (60× magnification); λ_g is the average globule diameter and back-scattered (SEM) images evidencing the eutectic mixture (interdendritic) and the dendritic matrix.

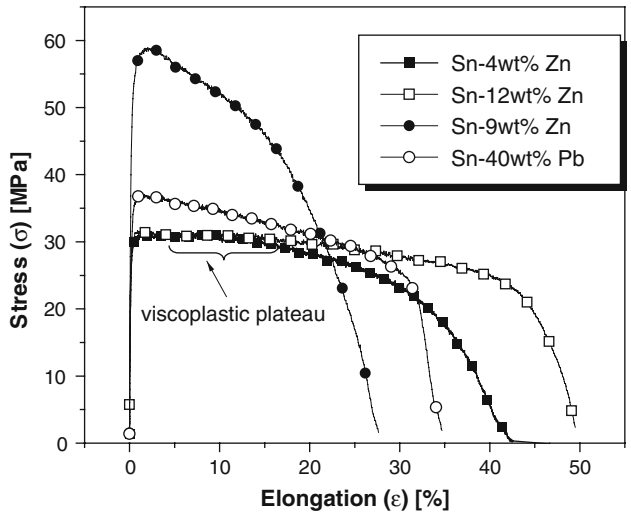

Fig. 12. Experimental stress–strain curves for: (a) Sn-4wt.%Zn, (b) Sn-12wt.%Zn, (c) Sn-9wt.%Zn, and (d) Sn-40wt.%Pb solder alloys.

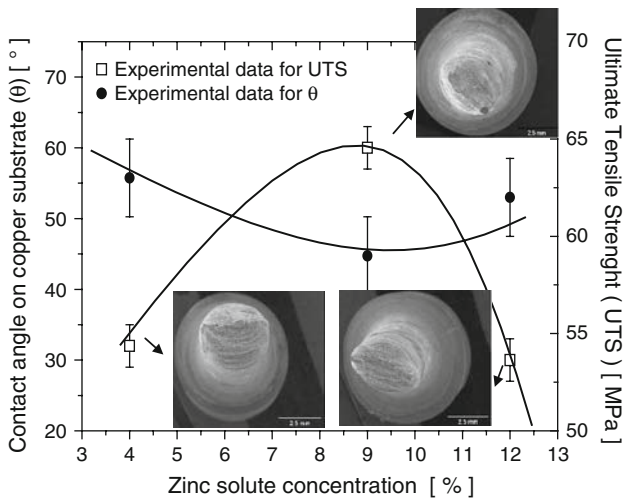

Fig. 13. Experimental results of contact angle on the copper substrate and ultimate tensile strength as a function of Zn content for Sn-Zn solder alloys, with corresponding fractographs.

Islam et al.[4] have recently reported that similar globular-like Zn-rich phase (spheroids) associated with a fine eutectic mixture increased the resulting hardness. The resulting globules or spheroids can hinder the movement of the dislocation lines, providing better mechanical behavior, as shown in Fig. 12. However, it was shown recently that, under low cooling rates during casting (about 0.5 °C/s), the resulting morphological pattern consists of needle-like Zn-rich phase distributed in the eutectic mixture,[34] and as a direct consequence the ultimate tensile strength decreases to about 40 MPa. In a needle-like Zn-rich phase, the dislocation lines can easily move across the lattice, decreasing hardness and tensile strength, as also reported by Islam et al.[4]

Figure 13 shows trend curves of ultimate tensile strength with corresponding fractographs and contact angle as a function of Zn content for Sn-Zn

alloys (samples obtained with a cooling rate of about 12°C/s and a soldering temperature of 250°C). It is well known that the great challenge in engineering applications is the improvement of a property without provoking deleterious effects in another property. It can be seen that, of the Sn-Zn alloys examined, the eutectic Sn-9wt.%Zn alloy offers a compromise between lower wettability and higher mechanical strength.

CONCLUSIONS

The contact angles on the Cu substrate for all alloys examined generally tend to attain their lowest values for a melt superheat of 100°C. However, based on the range of contact angles given by the error bars (maximum and minimum values), average values of about 59° and 48° can be considered for the three Sn-Zn alloys and the Sn-40wt.%Pb solder alloy, respectively. The average values of contact angles on both low-carbon steel and tin plate substrates for the Sn-4wt.%Zn, Sn-12wt.%Zn, and Sn-40wt.%Pb alloys do not seem to be significantly affected by the melt superheat. On the other hand, for the Sn-9wt.%Zn alloy, a decrease (of about 17%) on the contact angle at 100°C can be observed when compared with that attained for a 50°C melt superheat.

It was found that only the Sn-Pb solder alloy tends to have the covered layer thickness in a Cu substrate decreasing with increasing dipping temperature. All the Sn-Zn solder alloys experienced a slight increase in layer thickness with increasing dipping temperature. In the range of dipping temperatures between 230°C and 250°C, quite similar covered layer thicknesses were observed for all tested solder alloys.

It was found that, of all the experimentally examined alloys, the highest ultimate tensile strength (UTS) of about 60 MPa and the lowest elongation of about 30% were obtained for the Sn-9wt.%Zn alloy. This seems to be closely associated with the resulting microstructure, consisting of small globular-like Zn particles and the eutectic mixture which is a result of the high cooling rate imposed during solidification. Furthermore, for low-carbon steel and tin plate substrates the use of 100°C of melt superheat makes it possible to attain a contact angle of about 50°, which is quite close to that found for the classic Sn-40wt.%Pb solder alloy (about 48°).

The control of solder alloys by manipulating solidification processing variables, permitting the control of cooling rate, can be used as an alternative way to produce components with a compromise between reasonable wettability and good mechanical properties.

ACKNOWLEDGEMENTS

The authors acknowledge financial support provided by FAPESP (The Scientific Research Foundation of the State of São Paulo, Brazil), CNPq (The Brazilian Research Council) and FAEPEX-UNICAMP.

REFERENCES

1. S.P. Yu, H.J. Lin, and M.H. Hon, *J. Mater. Sci.: Mater. Electron.* 11, 461 (2000).
2. F.A. El-Salam, R.H. Nada, and A.M.A. El-Khalek, *Mater. Sci. Eng. A* 448, 171 (2007).
3. K. Suganuma and K.S. Kim, *J. Mater. Sci.: Mater. Electron.* 18, 121 (2007).
4. R.A. Islam, Y.C. Chan, W. Jillek, and S. Islam, *Microelectron. J.* 37, 705 (2006).
5. X. Chen, M. Li, X.X. Ren, A.M. Hu, and D.L. Mao, *J. Electron. Mater.* 35, 1734 (2006).
6. C. Wei, Y.C. Liu, Y.J. Han, J.B. Wan, and K. Yang, *J. Alloys Compd.* 464, 301 (2008).
7. K.L. Lin, K.I. Chen, H.M. Hsu, and C.L. Shi, *Electronic Components and Technology Conference* (2003), p. 658.
8. H. Wang, H. Zhao, D.P. Sekulic, and Y. Qian, *J. Electron. Mater.* 37, 1640 (2008).
9. J. Sylvestre and A. Blander, *J. Electron. Mater.* 37, 1618 (2008).
10. M. McCormack, S. Jin, H.S. Chen, and D.A. Machusak, *J. Electron. Mater.* 23, 687 (1994).
11. K.S. Kim, S.H. Huh, and K. Suganuma, *J. Alloys Compd.* 352, 226 (2003).
12. M. McCormack, S. Jin, G.W. Kammlott, and H.S. Chen, *Appl. Phys. Lett.* 63, 15 (1993).
13. C.M. Miller, I.E. Anderson, and J.F. Smith, *J. Electron. Mater.* 23, 595 (1994).
14. G. Montesperelli, M. Rapone, F. Nanni, P. Travaglia, P. Riani, R. Marazza, and G. Gusmano, *Mater. Corr.* 59, 662 (2008).
15. M. McCormack and S. Jin, *J. Electron. Mater.* 23, 635 (1994).
16. I. Shohji, C. Gagg, and W.J. Plumbridge, *J. Electron. Mater.* 33, 923 (2004).
17. A. Sharif and Y.C. Chan, *Microelectron. Eng.* 84, 328 (2007).
18. J. Madeni, S. Liu, and T. Siewert, *2nd International Brazing and Soldering Conference (ISBC)* (San Diego, California, 2003), February 17–19.
19. J.T. Berry, *AFS Trans.* 78, 421 (1970).
20. P. Donelan, *Mater. Sci. Technol.* 16, 261 (2000).
21. J.M. Quaresma, C.A. Santos, and A. Garcia, *Metall. Mater. Trans. A* 31, 3167 (2000).
22. W.R. Osório and A. Garcia, *Mater. Sci. Eng. A* 325, 103 (2002).
23. W.R. Osório, C.A. Santos, J.M.V. Quaresma, and A. Garcia, *J. Mater. Process. Technol.* 143, 703 (2003).
24. W.R. Osório, P.R. Goulart, G.A. Santos, C. Moura Neto, and A. Garcia, *Metall. Mater. Trans. A* 37, 2525 (2006).
25. W.R. Osório, J.E. Spinelli, N. Cheung, and A. Garcia, *Mater. Sci. Eng. A* 420, 179 (2006).
26. C.A. Siqueira, N. Cheung, and A. Garcia, *Metall. Mater. Trans. A* 33, 2107 (2002).
27. W.R. Osório, C.S.C. Aoki, and A. Garcia, *J. Power Sources* 185, 1471 (2008).
28. K. Suganuma, K. Niihara, T. Shoutoku, and Y. Nakamura, *J. Mater. Res.* 13, 2859 (1998).
29. C.M.L. Wu, C.M.T. Law, D.Q. Yu, and L. Wang, *J. Electron. Mater.* 32, 63 (2003).
30. C.M.L. Wu, D.Q. Yu, C.M.T. Law, and L. Wang, *Mater. Sci. Eng. R* 44, 1 (2004).
31. T.C. Toye and E.R. Jones, *Proc. Phys. Soc.* 71, 88 (1957).
32. S.C. Cheng and K.L. Lin, *J. Electron. Mater.* 31, 940 (2002).
33. D.M. Rosa, J.E. Spinelli, I.L. Ferreira, and A. Garcia, *Metall. Mater. Trans. A* 39, 2161 (2008).
34. X. Wei, H. Huang, L. Zhou, M. Zhang, and X. Liu, *Mater. Lett.* 61, 655 (2007).
35. M.C. Flemings, *Solidification Processing* (New York: McGraw Hill, 1974).

36. L.R. Garcia, L.C. Peixoto, W.R. Osório, and A. Garcia, *Mater. Lett.* 63, 1314 (2009).
37. S. Wiese and K. Wolter, *Microelectron. Reliab.* 44, 1923 (2004).
38. Y.S. Kim, K.S. Kim, C.W. Hwang, and K. Suganuma, *J. Alloys Compd.* 352, 233 (2003).
39. J.E. Lee, K.S. Kim, M. Inoue, J. Jiang, and K. Suganuma, *J. Alloys Compd.* 454, 310 (2008).